

INTERACTION OF BUOYANT PLUMES IN OPEN-CHANNEL FLOW

P. J. WICKS¹

(Received 1 January 1991; revised 24 April 1991)

Abstract

In this paper, a model for lateral dispersion in open-channel flow is studied involving a diffusion equation which has a nonlinear term describing the effect of buoyancy. The model is used to investigate the interaction of two buoyant pollutant plumes. An approximate analytic technique involving Hermite polynomials is applied to the resulting PDEs to reduce them to a system of ODEs for the centroids and widths of the two plumes. The ODEs are then solved numerically. A rich variety of behaviour occurs depending on the relative positions, widths and strengths of the initial discharges. It is found that for two plumes of equal strength and width discharged side-by-side, the plumes move apart and the rate of spreading is inhibited by their interaction, whereas when one plume is initially much wider than the other, both plumes tend to drift to the side of the narrower plume. Finally, the PDEs are solved numerically for two sets of initial conditions and a comparison is made with the ODE solutions. Agreement is found to be good.

1. Introduction

It is a common feature of pollutant discharges into rivers and estuaries that the pollutant has a different density to the water into which it is discharged. When this is the case, the pollutant is nonpassive, since its buoyancy causes stratification and secondary flow. An important example of this is thermal discharge, i.e. when the pollutant is warm water. A complete modelling of the dispersion of such a discharge requires us to examine the flow field in each of a number of different zones. Smith [4] identifies these zones for discharge in shallow water as (i) a near field, featuring vertical stratification

¹Depart. of Applied Maths and Theoretical Physics, University of Cambridge, UK.
© Copyright Australian Mathematical Society 1992, Serial-fee code 0334-2700/92

and the influence of outfall geometry, (ii) a middle field of vertically mixed flow which is spreading laterally, and (iii) a far field where the lateral mixing is almost complete. Buoyancy-driven secondary flow occurs in both the mid- and far-field. In certain situations (e.g. in rivers or in mid-tide estuary flow) the primary flow can be considered as steady and unidirectional.

The effect of buoyancy on midfield flow for this case has been studied experimentally and analytically by Prych [2]. He found that in the presence of density differences, a secondary flow is set up which enhances the lateral mixing process. Unfortunately, agreement between Prych's analysis and his experiments is not good. In response to this, Smith [4] carried out an analytic study in which some of the simplifying assumptions made by Prych are relaxed to include phenomena such as stratification and horizontal circulation. The following equation is derived in Smith's analysis as a limiting case in which all longitudinal derivatives are neglected with respect to axes moving with the bulk velocity:

$$\frac{\partial c}{\partial t} = \frac{\partial}{\partial y} \left[D_0 + D_2 \left(\frac{\partial c}{\partial y} \right)^2 \right] \frac{\partial c}{\partial y}, \quad (1.1)$$

where c is the depth-averaged concentration of contaminant, y is the lateral displacement and the coefficients D_0 and D_2 are given by

$$D_0 = 0.15hu_* \quad (1.2)$$

$$D_2 = 0.16h^5(\alpha g)^2/u_*^3, \quad (1.3)$$

h being the water depth, u_* the friction velocity, and αg the reduced gravity of the buoyant contaminant. This is the equation derived by Erdogan and Chatwin [1] in the context of longitudinal mixing in pipe flow. The dispersion coefficient has a nonconstant term proportional to the square of the concentration gradient, which quantifies the enhancement of lateral mixing due to buoyancy. Comparisons are shown in Smith [3] between predictions based on (1.1) and some of Prych's experiments in which secondary flow is the main mechanism for buoyancy-induced dispersion. These comparisons show much better agreement than that obtained by Prych.

When there are two discharges of the buoyant pollutant, it is convenient to regard the resulting plumes separately, even when the two pollutants are the same (e.g. hot water). Thus we require two equations, one each for the concentrations of the two pollutants, c_1 and c_2 . The nonconstant term in the dispersion coefficient will now be proportional to the sum of the

concentration gradients. Thus we arrive at a system of two coupled PDEs:

$$\frac{\partial c_1}{\partial t} = \frac{\partial}{\partial y} \left[D_0 + D_2 \left(\frac{\partial c_1}{\partial y} + \frac{\partial c_2}{\partial y} \right)^2 \right] \frac{\partial c_1}{\partial y} \quad (1.4a)$$

$$\frac{\partial c_2}{\partial t} = \frac{\partial}{\partial y} \left[D_0 + D_2 \left(\frac{\partial c_1}{\partial y} + \frac{\partial c_2}{\partial y} \right)^2 \right] \frac{\partial c_2}{\partial y}. \quad (1.4b)$$

On adding equations (1.4) and putting $c = c_1 + c_2$, the Erdogan-Chatwin equation is recovered.

In Section 2, scalings are introduced which nondimensionalise (1.4). The rest of this paper concerns the study of the dimensionless equations

$$\frac{\partial c_1}{\partial t} = \frac{\partial}{\partial y} \left[1 + \left(\frac{\partial c_1}{\partial y} + \frac{\partial c_2}{\partial y} \right)^2 \right] \frac{\partial c_1}{\partial y} \quad (1.5a)$$

$$\frac{\partial c_2}{\partial t} = \frac{\partial}{\partial y} \left[1 + \left(\frac{\partial c_1}{\partial y} + \frac{\partial c_2}{\partial y} \right)^2 \right] \frac{\partial c_2}{\partial y}. \quad (1.5b)$$

The limits of weak and strong nonlinearity are discussed for the one-plume case in Section 3, and the symmetric case for two plumes in Section 4. In Sections 5 and 6 an approximate analytic technique is presented resulting in a system of ODEs. These can be solved numerically more cheaply than can (1.5), and therefore several cases may be studied by varying the initial conditions to show the rich variety of behaviour that can occur. By studying these results and analysing the significance of some of the terms in the ODEs, much insight into the behaviour of the system is gained. This is done in Section 7. Since the analytic approach is applied to the dimensionless equations, comments concerning the range of validity of the ODE model apply equally to all situations for which the dimensionless times, distances and concentrations are the same. This range of validity is discussed in Section 8, where a comparison is made for two particular cases between the ODE model predictions and a full numerical solution of (1.5). Agreement is found to be excellent for an asymmetric case and fair for a symmetric case suggesting that the model is valid over a wide range.

2. Non-dimensionalisation

The total amount of pollutant discharged is represented by the quantity

$$M = \int_{-\infty}^{\infty} (c_1 + c_2) dy, \quad (2.1)$$

and is conserved by (1.4). We may normalise M , D_0 and D_2 to unity by nondimensionalising the equations with the following scalings:

$$T = (D_2 M^2 / D_0^3)^{1/2} \quad (2.2)$$

$$L = (D_0 T)^{1/2} \quad (2.3)$$

$$C = M/L. \quad (2.4)$$

We can therefore study without loss of generality the dimensionless equations (1.5), with initial conditions such that $M = 1$.

3. Limiting cases for a single species

In the case of just one plume, the equation to be solved is

$$\frac{\partial c}{\partial t} = \frac{\partial}{\partial y} \left[1 + \left(\frac{\partial c}{\partial y} \right)^2 \right] \frac{\partial c}{\partial y}. \quad (3.1)$$

Although this equation has not been solved analytically in general, there are solutions in the limiting cases where one or other of the terms in the dispersion coefficient dominates.

When concentration gradients are vanishingly small (the linear limit), we arrive at the linear diffusion equation. For this case, it has been shown that the concentration c eventually assumes a Gaussian profile as it proceeds downstream, with the lateral dimension increasing as $t^{1/2}$, regardless of the initial conditions. This can be shown by using the Hermite expansion

$$c = \frac{M}{\sqrt{2\pi}\sigma(t)} \sum_{n=0}^{\infty} \frac{a_n(t)}{n!} He_n(\eta) e^{-\eta^2/2} \quad (3.2)$$

with the deformed co-ordinate

$$\eta = y/\sigma(t), \quad (3.3a)$$

where

$$\sigma(t) = [2(t + t_0)]^{1/2}. \quad (3.3b)$$

If we take moments of the diffusion equation, the n th moment being formed by writing the diffusion equation in terms of the deformed co-ordinate, multiplying both sides of the diffusion equation by $He_n(\eta)$ and integrating over η , then a series of evolution equations is generated for the coefficients $a_n(t)$. It is found that the leading coefficient is conserved, whereas the other coefficients decay algebraically.

At the other extreme is the limit of *strong* nonlinearity, i.e. when the non-constant term is very large. For the one-plume case in this limit there is a similarity solution, derived in Smith [5], which takes the form

$$c = \frac{1.043M[1 - \eta^{4/3}]^{3/2}}{(52.25M^2t)^{1/6}} \quad (3.4)$$

with

$$\eta = \frac{y}{(52.25M^2t)^{1/6}}. \tag{3.5}$$

There are four things to be noted with regard to this solution. First, the lateral dimension increases as $t^{1/6}$ not $t^{1/2}$, so that for small times (when the nonlinear limit is valid) the solution spreads more rapidly than in the linear limit. Secondly, the solution is of finite extent, unlike the Gaussian solution of the linear limit. Thirdly, the solution supports singularities in the second derivative of concentration, both at the centre where $c \propto 1 - 3/2\eta^{4/3}$, and at the edges where $c \propto (1 - |\eta|)^{3/2}$. Fourthly, the rate of spreading depends on the source strength M , so that stronger plumes spread faster than weaker plumes. Note also that this limit is applicable when concentration gradients are very high; but in this case diffusion occurs rapidly with the effect of quickly reducing the gradients. Therefore the limit of strong nonlinearity is valid only on a short time-scale.

4. The symmetric case for two species

We shall be interested in the behaviour of the plume centroids $y_1(t)$ and $y_2(t)$ and the plume spreads $\sigma_1(t)$ and $\sigma_2(t)$, where

$$y_i(t) = \frac{\int_{-\infty}^{\infty} yc_i dy}{M_i} \tag{4.1}$$

$$\sigma_i^2(t) = \frac{\int_{-\infty}^{\infty} (y - y_i)^2 c_i dy}{M_i} \tag{4.2}$$

and M_i is the conserved quantity

$$\int_{-\infty}^{\infty} c_i dy, \quad i = 1, 2.$$

Equation (1.5a) gives the following evolution equation for y_1 :

$$\frac{dy_1}{dt} = -\frac{2}{M_1} \int_{-\infty}^{\infty} \left(\frac{\partial c_1}{\partial y}\right)^2 \frac{\partial c_2}{\partial y} dy - \frac{1}{M_1} \int_{-\infty}^{\infty} \frac{\partial c_1}{\partial y} \left(\frac{\partial c_2}{\partial y}\right)^2 dy. \tag{4.3}$$

For the symmetric case in which $c_1(y) = c_2(-y)$, the two terms in (4.3) have opposite sign, but the first term is twice as big as the second. Hence the

sign of the first term determines the sign of dy_1/dt . Typically this will be negative since $\partial c_1/\partial y$ is negative in the region of overlap. In this case the effect of interaction will be for the two plumes to move apart.

5. Hermite expansion for two species

We have seen from the one-plume case that at larger times the concentration profiles tend to become Gaussian. With this in mind, we now attempt to apply the Hermite expansion method mentioned in Section 3 to the two-plume equations (1.5). The deformed co-ordinates to be used are

$$\eta_1 = (y - y_1(t))/\sigma_1(t), \quad (5.1a)$$

$$\eta_2 = (y - y_2(t))/\sigma_2(t), \quad (5.1b)$$

where y_1 and y_2 are the centroids of the respective plumes, and σ_1^2 and σ_2^2 are the variances; $a_n(t)$ and $b_n(t)$ are the Hermite coefficients relating to the first and second plumes respectively. In the (t, η_1) co-ordinate system, (1.5a) becomes

$$\frac{\partial c_1}{\partial t} = \left(\frac{\eta_1}{2\sigma_1^2} \frac{d\sigma_1^2}{dt} + \frac{1}{\sigma_1} \frac{dy_1}{dt} \right) \frac{\partial c_1}{\partial \eta_1} + \frac{1}{\sigma_1^2} \frac{\partial}{\partial \eta_1} \left[1 + \frac{1}{\sigma_1^2} \left(\frac{\partial c_1}{\partial \eta_1} + \frac{\partial c_2}{\partial \eta_1} \right)^2 \right] \frac{\partial c_1}{\partial \eta_1}. \quad (5.2)$$

The n th Hermite component of this equation is then

$$\begin{aligned} \frac{d}{dt} \int_{-\infty}^{\infty} c_1 He_n(\eta_1) d\eta_1 &= -\frac{n+1}{2\sigma_1^2} \frac{d\sigma_1^2}{dt} \int_{-\infty}^{\infty} c_1 He_n(\eta_1) d\eta_1 \\ &\quad - \frac{n}{\sigma_1} \frac{dy_1}{dt} \int_{-\infty}^{\infty} c_1 He_{n-1}(\eta_1) d\eta_1 \\ &\quad + \frac{n(n-1)}{2\sigma_1^2} \left(2 - \frac{d\sigma_1^2}{dt} \right) \int_{-\infty}^{\infty} c_1 He_{n-2}(\eta_1) d\eta_1 \\ &\quad + \frac{1}{\sigma_1^4} \int_{-\infty}^{\infty} \frac{\partial}{\partial \eta_1} \left[\left(\frac{\partial c_1}{\partial \eta_1} + \frac{\partial c_2}{\partial \eta_1} \right)^2 \frac{\partial c_1}{\partial \eta_1} \right] He_n(\eta_1) d\eta_1. \end{aligned} \quad (5.3)$$

Substituting the Hermite series representations for c_1 and c_2 , and using the orthogonality properties of the Hermite polynomials gives

$$\begin{aligned} \left(\frac{d}{dt} + \frac{n}{2\sigma_1^2} \frac{d\sigma_1^2}{dt} \right) a_n &= -\frac{n}{\sigma_1} \frac{dy_1}{dt} a_{n-1} + \frac{n(n-1)}{2\sigma_1^2} \left(2 - \frac{d\sigma_1^2}{dt} \right) a_{n-2} \\ &\quad - \frac{1}{M_1 \sigma_1^3} I_n(t) \end{aligned} \quad (5.4)$$

where

$$I_0(t) = 0 \tag{5.5}$$

$$I_n(t) = \int_{-\infty}^{\infty} \frac{\partial}{\partial \eta_1} \left[\left(\frac{\partial c_1}{\partial \eta_1} + \frac{\partial c_2}{\partial \eta_1} \right)^2 \frac{\partial c_1}{\partial \eta_1} \right] He_n(\eta_1) d\eta_1 \quad \text{for } n = 1, 2, 3, \dots \tag{5.6}$$

The following evolution equations for y_1 and σ_1^2 are obtained from (5.4) by putting n equal to 1 and 2 respectively:

$$\frac{dy_1}{dt} = -\frac{1}{M_1 \sigma_1^2} I_1(t) \tag{5.7}$$

$$\frac{d\sigma_1^2}{dt} = 2 - \frac{1}{M_1 \sigma_1} I_2(t). \tag{5.8}$$

Evolution equations for y_2 and σ_2^2 are obtained similarly. Note that for this problem, $a_0(t)$ and $b_0(t)$ remain constant at unity for all t , i.e. the total amount of pollutant is conserved. The integrals $I_1(t)$ and $I_2(t)$ are calculated in the next section by way of a near-Gaussian approximation, which we expect to be good at moderate times when the nonlinear effects are not too great.

6. Calculation of $I_1(t)$ and $I_2(t)$

Using integration by parts on (5.6) gives

$$I_n(t) = -n \int_{-\infty}^{\infty} \left(\frac{\partial c_1}{\partial \eta_1} + \frac{\partial c_2}{\partial \eta_1} \right)^2 \frac{\partial c_1}{\partial \eta_1} He_{n-1}(\eta_1) d\eta_1. \tag{6.1}$$

In order to calculate $I_n(t)$ explicitly for $n = 1$ and 2 , we substitute once again the Hermite expansions for c_1 and c_2 . This yields three triply-infinite series involving triple products of the Hermite coefficients. Since our choice of deformed co-ordinates ensures that $a_1(t)$, $a_2(t)$, $b_1(t)$ and $b_2(t)$ are all identically zero, we may truncate each series after the leading term if we assume that the $a_i(t)$ and $b_i(t)$ are small for $i \geq 3$; this is the near-Gaussian approximation. We may then write

$$I_n(t) = -\frac{n}{(2\pi)^{3/2}} \int_{-\infty}^{\infty} \left(\frac{M_1}{\sigma_1} \eta_1 e^{-\eta_1^2/2} + \frac{\sigma_1 M_2}{\sigma_2^2} \eta_2 e^{-\eta_2^2/2} \right)^2 \cdot \frac{M_1}{\sigma_1} \eta_1 e^{-\eta_1^2/2} He_{n-1}(\eta_1) d\eta_1. \tag{6.2}$$

Thus

$$\begin{aligned}
 I_1 &= -\frac{1}{(2\pi)^{3/2}} \int_{-\infty}^{\infty} \left(\frac{M_1}{\sigma_1} \eta_1 e^{-\eta_1^2/2} + \frac{\sigma_1 M_2}{\sigma_2^2} \eta_2 e^{-\eta_2^2/2} \right)^2 \frac{M_1}{\sigma_1} \eta_1 e^{-\eta_1^2/2} d\eta_1 \\
 &= -\frac{M_1}{\sigma_1 (2\pi)^{3/2}} \left(J_1^{(1)}(t) + J_1^{(2)}(t) + J_1^{(3)}(t) \right), \tag{6.3}
 \end{aligned}$$

$$J_1^{(1)}(t) = \frac{M_1^2}{\sigma_1^2} \int_{-\infty}^{\infty} \eta_1^3 e^{-3\eta_1^2/2} d\eta_1 = 0, \tag{6.4}$$

$$J_1^{(2)}(t) = \frac{2M_1 M_2}{\sigma_2^2} \int_{-\infty}^{\infty} \eta_1^2 \eta_2 e^{-(2\eta_1^2 + \eta_2^2)/2} d\eta_1, \tag{6.5}$$

and

$$J_1^{(3)}(t) = \frac{M_2^2 \sigma_1^2}{\sigma_2^4} \int_{-\infty}^{\infty} \eta_1 \eta_2^2 e^{-(\eta_1^2 + 2\eta_2^2)/2} d\eta_1. \tag{6.6}$$

Further analysis gives

$$\begin{aligned}
 J_1^{(2)}(t) &= \frac{2M_1 M_2}{\sigma_2^2} \exp[-\Delta^2 / (\sigma_1^2 + 2\sigma_2^2)] \left(\frac{2\pi}{2 + \sigma_R^2} \right)^{1/2} \\
 &\quad \cdot \left(\frac{2\sigma_2 \Delta (\sigma_1^2 - \sigma_2^2)}{(\sigma_1^2 + 2\sigma_2^2)^2} - \frac{2\sigma_1^2 \sigma_2 \Delta^3}{(\sigma_1^2 + \sigma_2^2)^3} \right) \tag{6.7}
 \end{aligned}$$

$$\begin{aligned}
 J_1^{(3)}(t) &= \frac{M_2^2 \sigma_1^2}{\sigma_2^4} \exp[-\Delta^2 / (\sigma_1^2 + 2\sigma_2^2)] \left(\frac{2\pi}{1 + 2\sigma_R^2} \right)^{1/2} \\
 &\quad \cdot \left(\frac{2\sigma_1 \Delta (\sigma_1^2 - \sigma_2^2)}{(2\sigma_1^2 + \sigma_2^2)^2} + \frac{2\sigma_1 \sigma_2^2 \Delta^3}{(2\sigma_1^2 + \sigma_2^2)^3} \right) \tag{6.8}
 \end{aligned}$$

where $\Delta = y_2 - y_1$ and $\sigma_R = \sigma_1 / \sigma_2$. Similarly

$$\begin{aligned}
 I_2(t) &= -\frac{2}{(2\pi)^{3/2}} \int_{-\infty}^{\infty} \left(\frac{M_1}{\sigma_1} \eta_1 e^{-\eta_1^2/2} + \frac{\sigma_1 M_2}{\sigma_2^2} \eta_2 e^{-\eta_2^2/2} \right)^2 \frac{M_1}{\sigma_1} e^{-\eta_1^2/2} \eta_1 d\eta_1 \\
 &= -\frac{2M_1}{\sigma_1 (2\pi)^{3/2}} \left(J_2^{(1)}(t) + J_2^{(3)}(t) + J_2^{(3)}(t) \right), \tag{6.9}
 \end{aligned}$$

where

$$J_2^{(1)} = \frac{M_1^2}{\sigma_1^2} \int_{-\infty}^{\infty} \eta_1^4 e^{-3\eta_1^2/2} d\eta_1 = \frac{1}{3} \left(\frac{2\pi}{3} \right)^{1/2} \frac{M_1^2}{\sigma_1^2}, \tag{6.10}$$

$$J_2^{(2)}(t) = \frac{2M_1M_2}{\sigma_2^2} \int_{-\infty}^{\infty} \eta_1^3 \eta_2 e^{-(2\eta_1^2 + \eta_2^2)/2} d\eta_1, \tag{6.11}$$

and

$$J_2^{(3)}(t) = \frac{M_2^2 \sigma_1^2}{\sigma_2^4} \int_{-\infty}^{\infty} \eta_1^2 \eta_2^2 e^{-(\eta_1^2 + 2\eta_2^2)/2} d\eta_1. \tag{6.12}$$

Further analysis gives

$$J_2^{(2)} = \frac{2M_1M_2}{\sigma_2^2} \exp[-\Delta^2 / (\sigma_1^2 + 2\sigma_2^2)] \left(\frac{2\pi}{2 + \sigma_R^2} \right)^{1/2} \cdot \left(\frac{3\sigma_1\sigma_2^3}{(\sigma_1^2 + 2\sigma_2^2)^2} + \frac{3\sigma_1\sigma_2\Delta^2(\sigma_1^2 - 2\sigma_2^2)}{(\sigma_1^2 + 2\sigma_3^2)^3} - \frac{2\sigma_1^3\sigma_2\Delta^4}{(\sigma_1^2 + 2\sigma_2^2)^4} \right) \tag{6.13}$$

$$J_2^{(3)}(t) = \frac{M_2^2 \sigma_1^2}{\sigma_2^4} \exp[-\Delta^2 / (\sigma_1^2 + 2\sigma_2^2)] \left(\frac{2\pi}{1 + 2\sigma_R^2} \right)^{1/2} \cdot \left(\frac{3\sigma_1^2\sigma_2^2}{(2\sigma_1^2 + \sigma_2^2)^2} + \frac{\Delta^2(4\sigma_1^4 + 8\sigma_1^2\sigma_2^2 + \sigma_2^4)}{(2\sigma_1^2 + \sigma_2^2)^3} + \frac{4\sigma_1^2\sigma_2^2\Delta^4}{(2\sigma_1^2 + \sigma_2^2)^4} \right). \tag{6.14}$$

Substitution into the evolution equations (5.7) and (5.8) gives, along with the analogous results for y_2 and σ_2^2 , a closed system of four ODEs which can be solved numerically.

7. Discussion and numerical solution of the ODEs

In the evolution equations (5.7) and (5.8), the integrals $I_1(t)$ and $I_2(t)$ quantify the effect of the nonlinearity. In order to understand the physical significance of the terms in these integrals, and the type of behaviour that ensues, some particular cases have been studied. The equations have also been solved numerically using a NAG routine, and results for the various cases are shown and discussed.

All but one of the terms in these integrals is proportional to an exponential involving the ratio of the separation Δ to some combination of the spreads σ_1 and σ_2 . If this ratio is large, these terms become exponentially small. The term that does not depend on Δ is $J_2^{(1)}(t)$. This term describes the effect of the nonlinearity on one plume in isolation; in other words, it does not involve the interaction of the two plumes. When only this term is included, the equations reduce to the one-plume evolution equation for the spread σ_1 described in Smith [3]. In the strong nonlinear limit this gives

$$\frac{d\sigma_1^2}{dt} \propto \frac{1}{\sigma_1^4},$$

and therefore the same $t^{1/6}$ power law as in the similarity solution.

Interesting two-plume behaviour thus occurs when the separation Δ is not too big. We consider separately cases of zero initial separation and non-zero initial separation. When there is no initial separation, the integral $I_1(t)$ is zero, so the plume centroids do not deviate and Δ remains zero for all time. Figure 1 shows numerical results for the case of two plumes of equal strength, and no separation. The excess variance plotted is found by calculating the variance σ_1^2 of the first plume in the presence of the second, and then subtracting the variance it would have if the second plume was absent. As Figure 1 shows, the growth of the excess variance depends on the relative initial plume widths (where the expression ‘plume width’ refers to the square root of the variance). When the initial plume widths are comparable, the excess variance grows rapidly at small times, and then levels off to a constant value at larger times, when the plumes have become sufficiently wide for linear diffusion to dominate. The behaviour is identical when the second plume is initially narrower, since the plume widths then equalise on a time-scale smaller than that on which the first plume is spreading. When the second plume is much wider, however, the initial growth of excess variance is reduced, and the final value is correspondingly less. In terms of the ODEs, the case of equal initial plume widths is identical to a one-plume case, and it may easily be shown that $I_2(t)$ has the same form as in the limit of large Δ but with M_1 replaced by $M_1 + M_2$.

The excess variance in this case is due to the increased overall source strength leading to higher concentration gradients. However when σ_2 is initially much larger than σ_1 , the concentration gradients associated with the second plume are initially much smaller, and the effect of the second plume on the spread of the first at small times is slight until the plume widths have

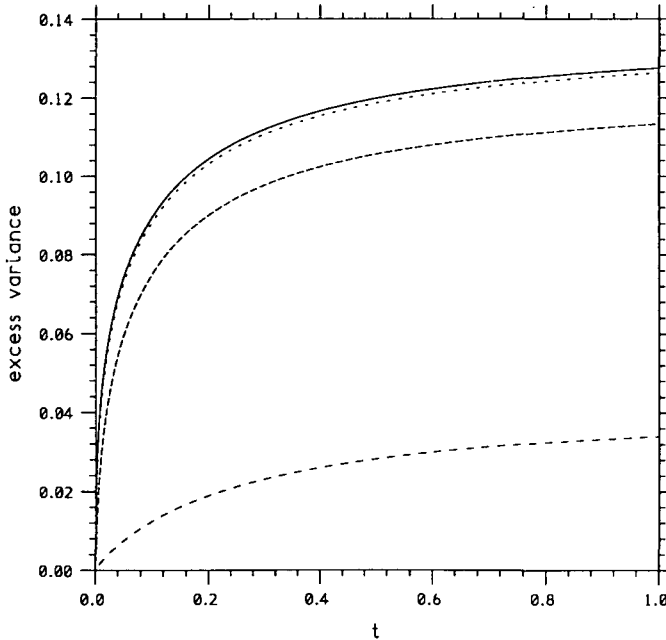


FIGURE 1. Excess variance of first plume due to presence of second plume
 $M_1 = 0.5$, $M_2 = 0.5$, $\Delta(0) = 0$, $\sigma_1^2(0) = 10^{-4}$
 $\sigma_2^2(0) = 10^{-4}$ (—), 0.02 (\cdots), 0.1 (---) and 1.0 (- - -).

equalised. This accounts for the reduced initial growth. Figures 2 (page 462) and 3 (page 463) show similar results for cases of unequal plume strengths. Results are similar, but it can be seen that the effect of the second plume is greater when its strength relative to the first is greater (Figure 3).

When there is initial separation, the behaviour may be expected to be different since the plumes may move away from or towards each other. Some results for $M_1 = M_2$ and $\Delta(t_0) = 0.2$ are shown in Figures 4a-d (pages 464–465). Figures 4a and 4b are plots of the plumes centroids and excess variance respectively against time, for various initial second plume widths; in Figures 4c and 4d the same data is plotted against logarithmic time axes to show the smalltime behaviour more clearly. The results can be interpreted as a transition between the following three cases.

When both initial plume widths are much smaller than the initial separation, the plume widths equalise before the plumes overlap significantly, so

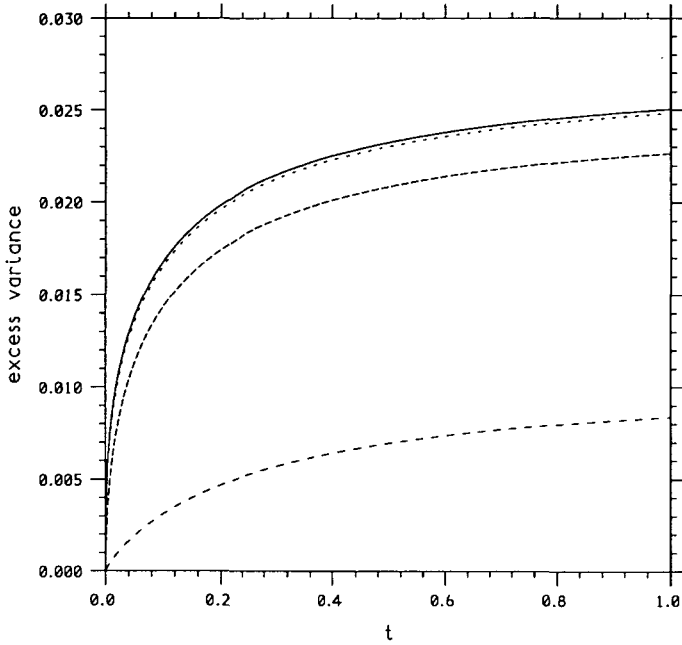


FIGURE 2. Excess variance of first plume due to presence of second plume

$$M_1 = 0.9, \quad M_2 = 0.1, \quad \Delta(0) = 0, \quad \sigma_1^2(0) = 10^{-4}$$

$$\sigma_2^2(0) = 10^{-4} \text{ (—), } 0.02 \text{ (···), } 0.1 \text{ (---) and } 1.0 \text{ (-.-).}$$

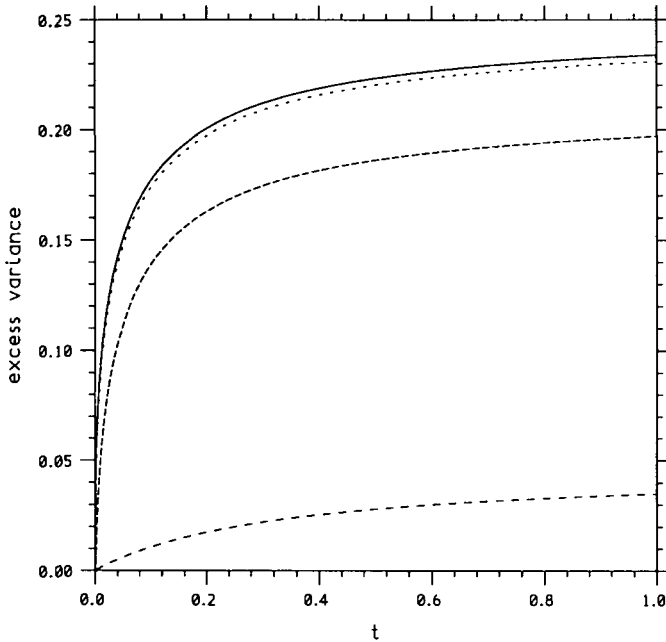


FIGURE 3. Excess variance of first plume due to presence of second plume

$$M_1 = 0.1, \quad M_2 = 0.9, \quad \Delta(0) = 0, \quad \sigma_1^2(0) = 10^{-4}$$

$$\sigma_2^2(0) = 10^{-4} \text{ (—), } 0.02 \text{ (}\cdots\text{)}, 0.1 \text{ (- - -)} \text{ and } 1.0 \text{ (- \cdot -)}.$$

we have the symmetric case studied in Section 4, and it can easily be shown that $I_1(t)$ is always positive so that the two plumes move apart in agreement with the result obtained in that section. A plausible explanation for this effect is that, when the plumes are beginning to overlap, the concentration gradients due to the two plumes in the space between them cancel out leading to low combined concentration gradients and low diffusion rates there, whereas diffusion rates on the outward side of each plume are hardly affected by the other. Since the overall diffusion is reduced, the excess variance goes negative, until the plumes merge sufficiently for diffusion to be enhanced. When one of the initial plume widths is increased beyond the value of the initial separation, the plumes overlap before their widths have had time to equalise. In this case the centroid of the wider plume moves *towards* the narrower plume, and the growth of the excess variance is more in line with the results of Figure 1. It would seem that the small region of relatively high concentration gradients on the nearer side of the wider plume increases the rate of diffusion there, giving an overall flux of concentration towards the other plume. The narrower plume moves away, however, since the gradient from the wider plume enhances diffusion on the far side of the narrower

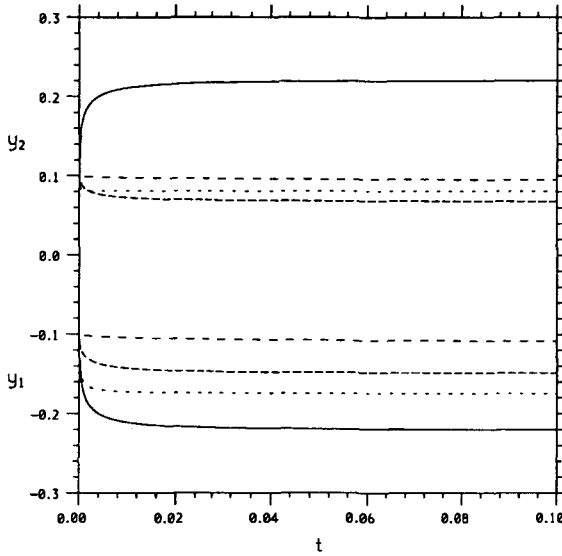


FIGURE 4a. Plume centroids of first plume due to presence of second plume

$$M_1 = 0.5, M_2 = 0.5, \Delta(0) = 0.2, \sigma_1^2(0) = 10^{-4}$$

$$\sigma_2^2(0) = 10^{-4} \text{ (—), } 0.02 \text{ (}\cdot\cdot\cdot\text{)}, 0.1 \text{ (- - -)} \text{ and } 1.0 \text{ (- - -)}.$$

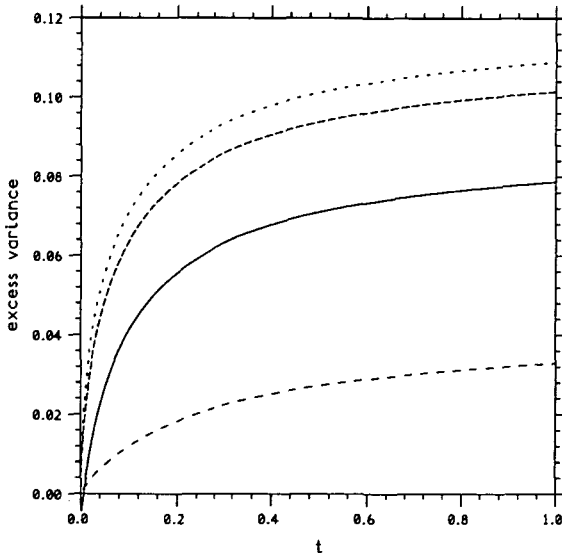


FIGURE 4b. Excess variance of first plume due to presence of second plume

$$M_1 = 0.5, M_2 = 0.5, \Delta(0) = 0.2, \sigma_1^2(0) = 10^{-4}$$

$$\sigma_2^2 = 10^{-4} \text{ (—), } 0.02 \text{ (}\cdot\cdot\cdot\text{)}, 0.1 \text{ (- - -)} \text{ and } 1.0 \text{ (- - -)}.$$

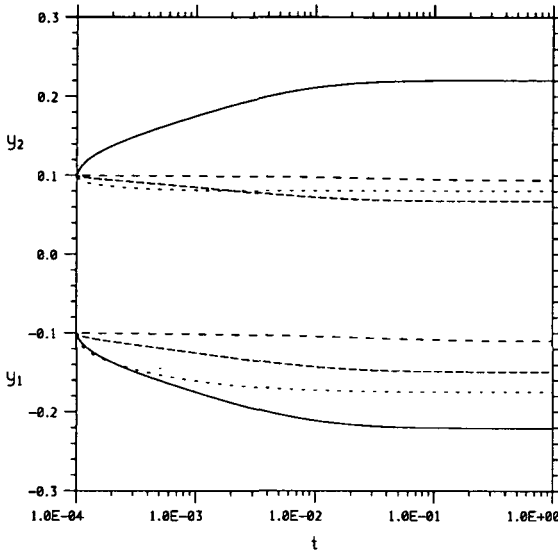


FIGURE 4c. Plume centroids against logarithmic time
 $M_1 = 0.5$, $M_2 = 0.5$, $\Delta(0) = 0.2$, $\sigma_1^2(0) = 10^{-4}$
 $\sigma_2^2 = 10^{-4}$ (—), 0.02(···), 0.1 (---) and 1.0 (-.-).

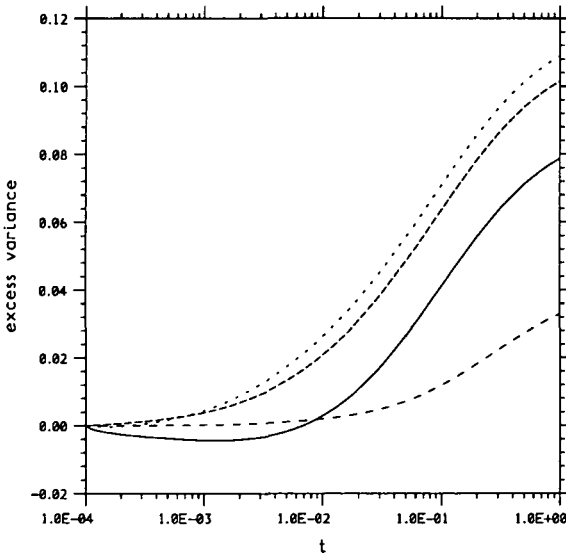


FIGURE 4d. Excess variance against logarithmic time
 $M_1 = 0.5$, $M_2 = 0.5$, $\Delta(0) = 0.2$, $\sigma_1^2(0) = 10^{-4}$
 $\sigma_2^2(0) = 10^{-4}$ (—), 0.02(···), 0.1 (---) and 1.0 (-.-).

plume. Finally, when one of the initial plume widths is of order 1 or greater (in nondimensional units), the concentration gradients associated with it become too small for significant nonlinear interaction to occur.

Figures 5a-d and 6a-d (pages 468–470) show results for unequal plume strengths. In Figures 5a-d, the first plume is stronger, so the excess variance takes much smaller values, and the centroid of the first plume deviates little. Much of the behaviour is similar to that shown in Figures 4a-d, but there are some significant differences. In the case of equal initial plume widths, the centroid of the second (weaker) plume deviates less than either plume in the equal strength case, because the concentration gradients in between the plumes do not cancel out to the same extent. Indeed, Figure 5c reveals that at very small times the weaker plume moves towards the stronger one; this is presumably a result of interaction with the tail of the stronger plume. In Figures 6a-d, the second plume is stronger, so the excess variance takes larger values and it is the first plume that deviates significantly; the case in which the stronger plume has an initial variance of 0.1 exhibits greater centroid deviation than in other figures.

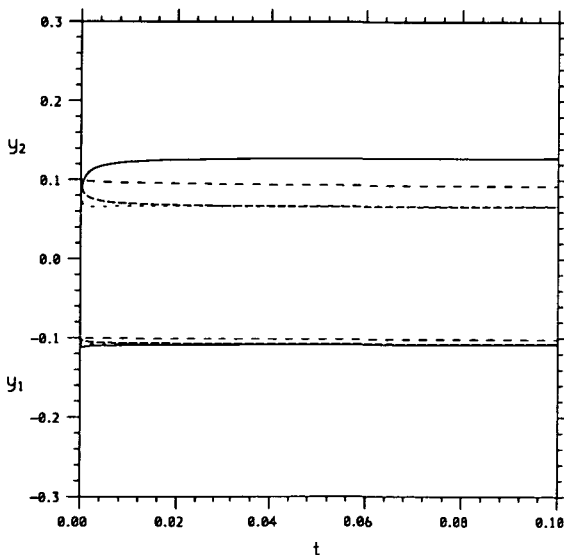


FIGURE 5a. Plume centroids of first plume due to presence of second plume

$$M_1 = 0.9, \quad M_2 = 0.1, \quad \Delta(0) = 0.2, \quad \sigma_1^2(0) = 10^{-4}$$

$$\sigma_2^2(0) = 10^{-4}(\text{---}), \quad 0.02(\cdots), \quad 0.1(\text{---}) \quad \text{and} \quad 1.0(\text{---}).$$

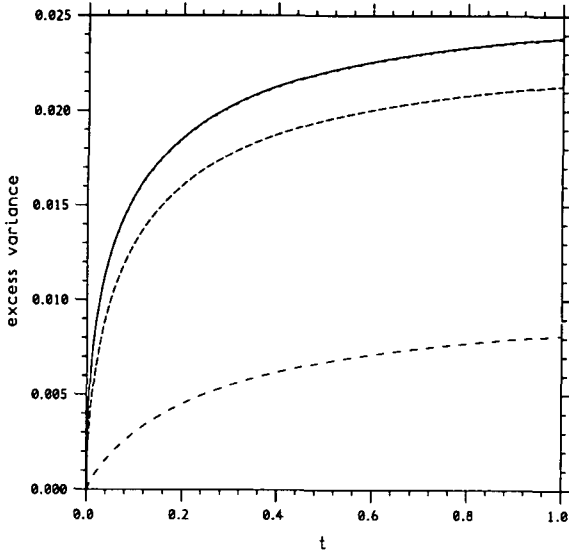


FIGURE 5b. Excess variance of first plume due to presence of second plume

$M_1 = 0.9, M_2 = 0.1, \Delta(0) = 0.2, \sigma_1^2(0) = 10^{-4}$
 $\sigma_2^2(0) = 10^{-4}$ (—), 0.02(· · ·), 0.1(---) and 1.0(- · -).

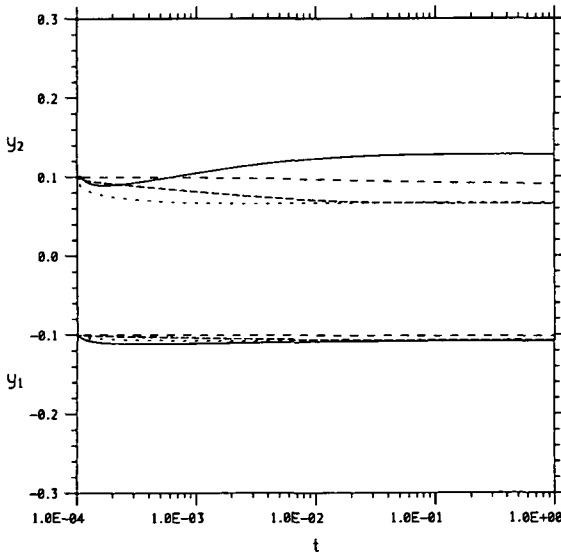


FIGURE 5c. Plume centroids against logarithmic time

$M_1 = 0.9, M_2 = 0.1, \Delta(0) = 0.2, \sigma_1^2(0) = 10^{-4}$
 $\sigma_2^2(0) = 10^{-4}$ (—), 0.02(· · ·), 0.1(---) and 1.0(- · -).

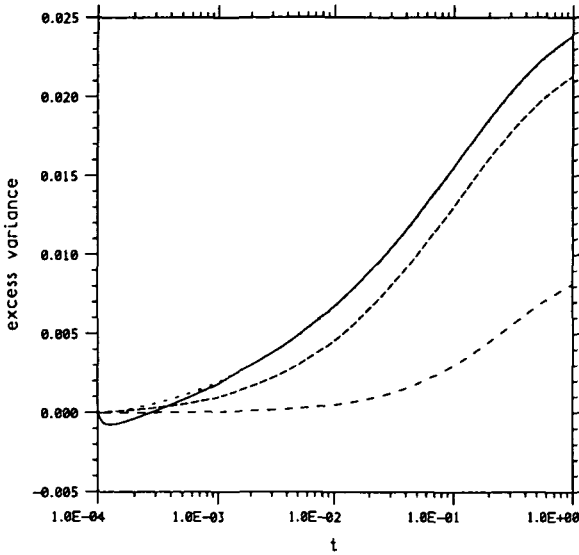


FIGURE 5d. Excess variance against logarithmic time
 $M_1 = 0.9, M_2 = 0.1, \Delta(0) = 0.2, \sigma_1^2(0) = 10^{-4}$
 $\sigma_2^2(0) = 10^{-4}(-), 0.02(\cdot\cdot\cdot), 0.1(- - -)$ and $1.0(- \cdot - \cdot -)$.

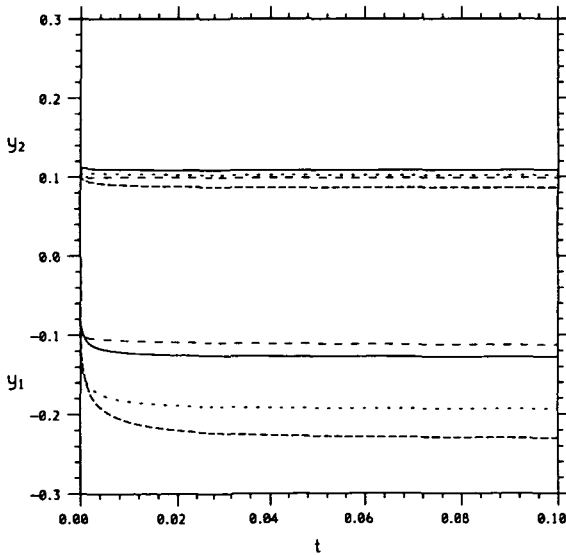


FIGURE 6a. Plume centroids of first plume due to presence of second plume
 $M_1 = 0.1, M_2 = 0.9, \Delta(0) = 0.2, \sigma_1^2(0) = 10^{-4}$
 $\sigma_2^2(0) = 10^{-4}(-), 0.02(\cdot\cdot\cdot), 0.1(- - -)$ and $1.0(- \cdot - \cdot -)$.

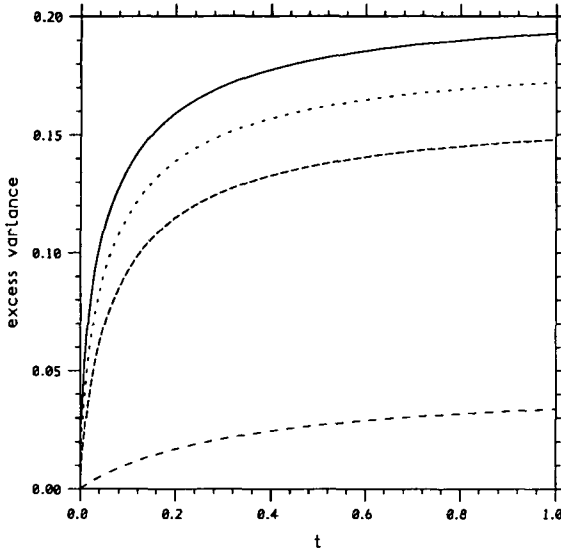


FIGURE 6b. Excess variance of first plume due to presence of second plume

$M_1 = 0.1, M_2 = 0.9, \Delta(0) = 0.2, \sigma_1^2(0) = 10^{-4}$
 $\sigma_2^2(0) = 10^{-4}$ (—), 0.02 (\cdots), 0.1 (- - -) and 1.0 (- · - ·).

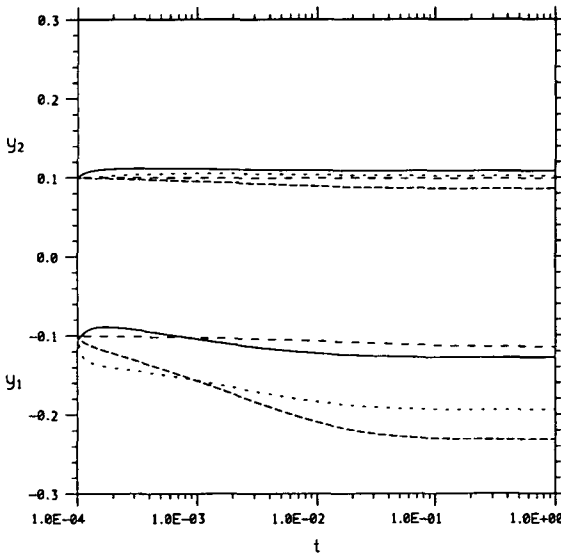


FIGURE 6c. Plume centroids against logarithmic time

$M_1 = 0.1, M_2 = 0.9, \Delta(0) = 0.2, \sigma_1^2(0) = 10^{-4}$
 $\sigma_2^2(0) = 10^{-4}$ (—), 0.02 (\cdots), 0.1 (- - -) and 1.0 (- · - ·).

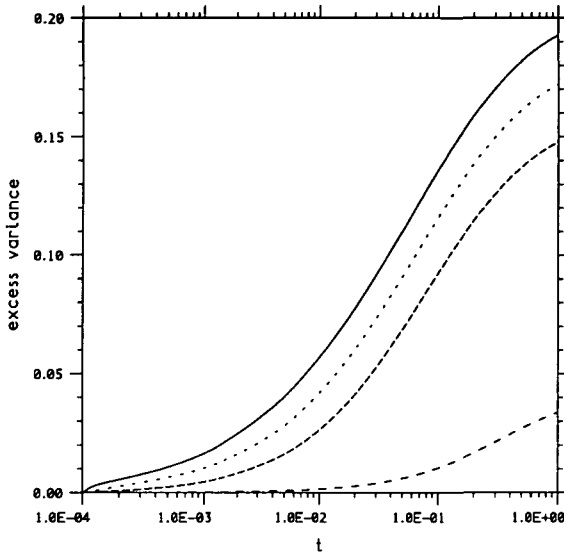


FIGURE 6d. Excess variance against logarithmic time
 $M_1 = 0.1$, $M_2 = 0.9$, $\Delta(0) = 0.2$, $\sigma_1^2(0) = 10^{-4}$
 $\sigma_2^2(0) = 10^{-4}$ (—), 0.02 (\cdots), 0.1 (- - -) and 1.0 (- · -).

8. Numerical solution of the PDEs: Comparison of results

The approximation made in Section 6 is based on the assumption that the nonlinearity of (1.5) causes the concentration profiles to deviate only slightly from Gaussian. One would expect this to be a good approximation when the nonlinear term is not strong compared to the linear term, i.e. when the nondimensional concentration gradients are not particularly high. However even when the nonlinear term is dominant, Smith [5] has shown that the rate of spreading of the similarity solution for the one-plume case of Section 3 and that predicted by the ODE model differs by only 3 or 4 percent.

In the two-plume case, skewness may arise if diffusion is inhibited locally by the concentration gradients having opposite sign. Equations (1.5) are solved numerically by using distorted co-ordinates based on the similarity solution of Section 3. The Crank-Nicholson method yields nonlinear difference equations which are solved iteratively at each time-step using the Newton-Raphson method.

Figures 7 and 8 (page 472) show snapshots of the concentration profiles of the PDE solutions at times when the nonlinear term is still significant but not overwhelming. Figure 7 shows an asymmetric case in which the centroids move to one side; Figure 8 shows a symmetric case in which the centroids move apart. The results are compared with Gaussian solutions based on the centroids and widths predicted by the ODE model. Figure 7 shows excellent agreement even at quite a small time. The inward side of the wider plume is wavy, due to the sharp variations in the diffusion coefficient over that region, but the Gaussian profile nevertheless fits remarkably well. Agreement is also good in the symmetric case of Figure 8 for a larger time, although there is considerable skewness arising from low values of the diffusion coefficient in between the centroids. At smaller times when the nonlinear term is still dominant, agreement is less good. These results suggest that for asymmetric cases where the concentration gradients of the two plumes do not cancel, the analytic approach has a very wide range of validity and the qualitative phenomena discussed in Section 7 are accurately preserved. For the

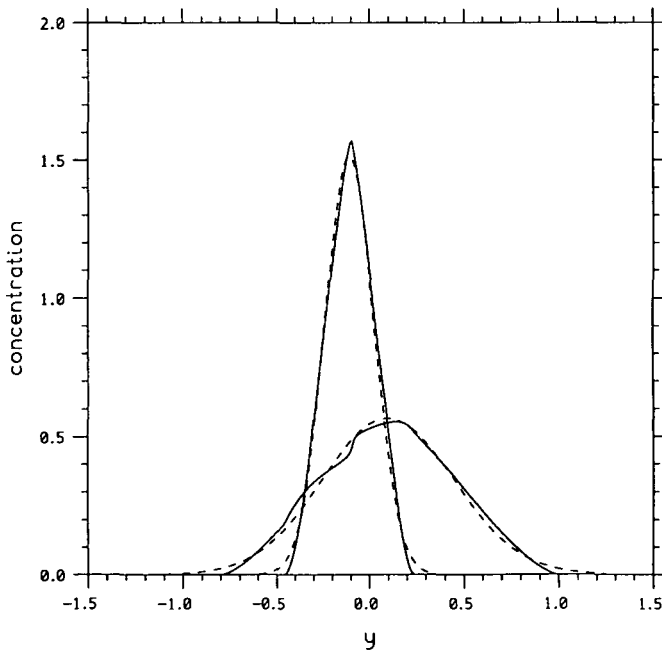


FIGURE 7. Comparison of a numerical solution of the p.d.e.'s (—) with results obtained from the o.d.e. model (- - -) at time $t = 10^{-4}$ with $M_1 = 0.5$, $M_2 = 0.5$, $\Delta(0) = 0.2$, $\sigma_1^2(0) = 10^{-4}$ and $\sigma_2^2(0) = 10^{-4}$.

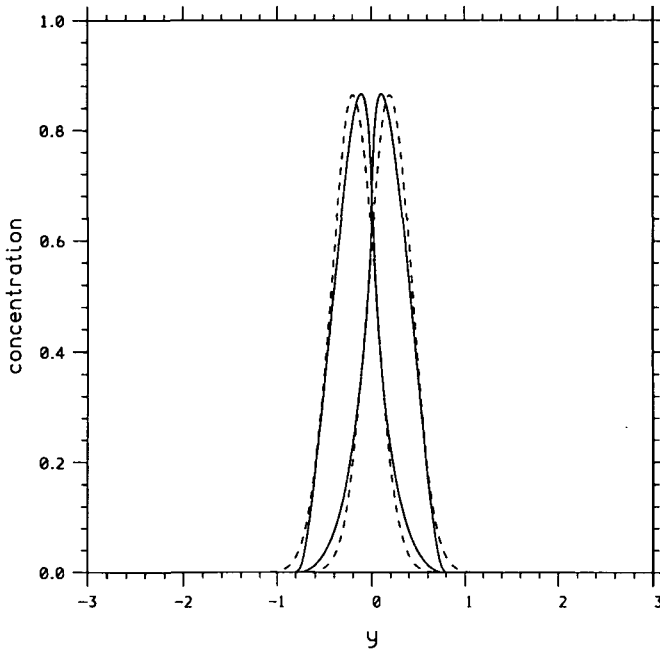


FIGURE 8. Comparison of a numerical solution of the p.d.e.'s (—) with results obtained from the o.d.e. model (- - -) at time $t = 3.16 * 10^{-3}$ with $M_1 = 0.5$, $M_2 = 0.5$, $\Delta(0) = 0.2$, $\sigma_1^2(0) = 10^{-4}$ and $\sigma_2^2(0) = 0.1$.

symmetric case, the model is valid in downstream areas where the dimensionless concentration gradients are at most of order unity.

9. Conclusions

An analytic method has been used to reduce a PDE model for buoyancy-affected dispersion to a system of ODEs, via an approximation involving the assumption that the concentration profiles remain Gaussian. Although this assumption ignores some of the possible behaviour, e.g. skewness of the profiles, the agreement demonstrated above is sufficient for considerable insight to be gained. The ODE model reveals that nonlinear interactions between the plumes give rise to a rich variety of behaviour which depends critically on the initial conditions.

10. Acknowledgement

The author wishes to thank National Power for their financial support.

References

- [1] M. E. Erdogan and P. C. Chatwin, "The effect of curvature and buoyancy on the laminar dispersion of solute in a horizontal tube", *J. Fluid Mech.* **29** (1967) 465–481.
- [2] E. A. Prych, "Effects of density differences on lateral mixing in open channel flows", *Keck Lab. Hydraul. Water Resources, Calif. Inst. Tech. Rep. KH-R-21* (1970).
- [3] R. Smith, "Asymptotic solutions of the Erdogan-Chatwin equation", *J. Fluid Mech.* **88** (1978) 323–337.
- [4] R. Smith, "Buoyancy effects upon lateral dispersion in open-channel flow", *J. Fluid Mech.* **90** (1979) 761–779.
- [5] R. Smith, "Similarity solutions of a non-linear diffusion equation", *IMA J. Appl. Math.* **28** (1982) 149–160.